VIP Electrochemical Imaging

DOI: 10.1002/anie.201200564

Definitive Evidence for Fast Electron Transfer at Pristine Basal Plane Graphite from High-Resolution Electrochemical Imaging**

*Stanley C. S. Lai, Anisha N. Patel, Kim M^cKelvey, and Patrick R. Unwin**

There is presently intense activity in electrochemical applications of novel sp^2 carbon materials, such as carbon nanotubes[1] and graphene,[2] which has led to a resurgence of interest in the intrinsic electrochemical properties of highly oriented pyrolytic graphite (HOPG), to which these materials are often compared.[1] The traditional consensus, deduced mostly from macroscopic cyclic voltammetry measurements (typically on areas $>0.1\ cm^2$) is that the electron transfer (ET) activity of HOPG is dominated by the step edges,[1,2g,3] with the basal plane showing very low[4] to no[5] electroactivity. However, the scale of these measurement necessarily means that HOPG basal planes and step edges are probed simultaneously,[3a,4,6] making it difficult to separate their individual reactivities. Furthermore, there are significant variations in reported HOPG electroactivity,[1c,3a–c,4–7] which has been attributed to each HOPG cleaved surface showing different quality (primarily step edge density). Consequently, various methods have been proposed to determine the step or defect density of cleaved HOPG.[1c,3a–c,4–7] However, the methods used hitherto are either microscopic and can only access a tiny fraction of the surface that is probed by macroscopic electrochemistry,[7c,d,8] or are indirect measurements of surface quality,[4,6b,c,7d] making it difficult to correlate HOPG surface structure and ET activity.

Here, we report significant advances in the newly developed technique scanning electrochemical cell microscopy (SECCM).[9] This technique greatly extends on the capabilities of previous scanning droplet based techniques,[10] allowing spatially resolved electrochemical imaging on a scale where the HOPG basal plane can be studied directly in isolation from step edges, and where the response also informs on the location of the measurement (basal surface vs. step edge). By further correlating high-resolution electrochemical measurements with atomic force microscope (AFM) images over the same area, we show unambiguously that the HOPG basal plane supports fast ET activity and conclude that the present (textbook)[11] model for the electroactivity of carbon-based materials requires radical revision.

The SECCM system is shown schematically in Figure 1a and is discussed in detail elsewhere.[9] In brief, a dual-channel glass capillary was pulled to a sharp point (300–400 nm; Figure 1b). Each channel was filled with an aqueous electrolyte solution and an Ag/AgCl quasi-reference counter electrode (QRCE). The liquid meniscus at the end of the pipet was brought into gentle contact with the HOPG sample,

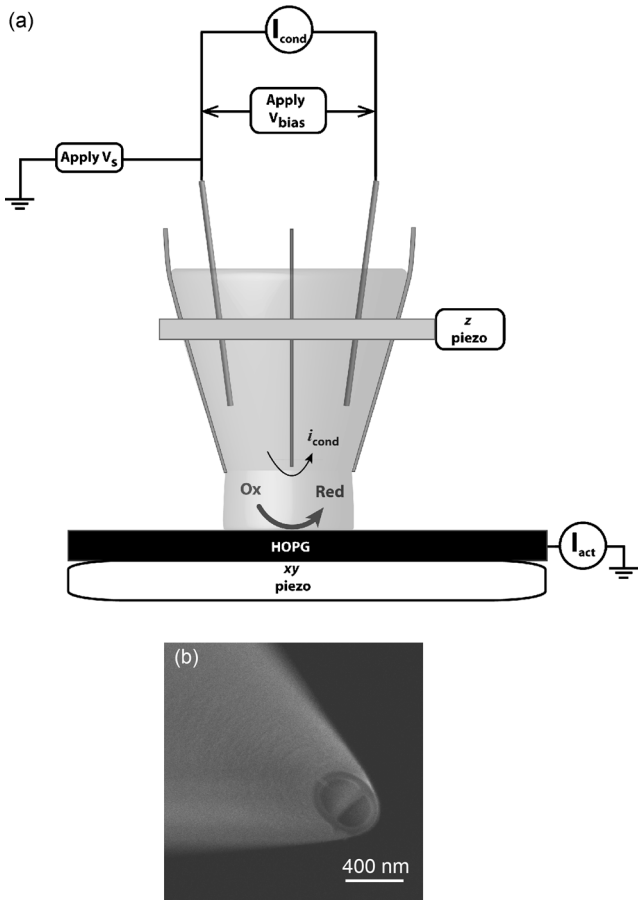

Figure 1. a) Schematic of the scanning electrochemical cell microscopy (SECCM) set-up. b) SEM image of the end of a pipet.

[*] Dr. S. C. S. Lai,[+] A. N. Patel,[+] K. M^cKelvey, Prof. Dr. P. R. Unwin
Department of Chemistry, University of Warwick
Coventry CV4 7AL (UK)
E-mail: p.r.unwin@warwick.ac.uk
K. M^cKelvey
MOAC doctoral training centre, University of Warwick
Coventry CV4 7AL (UK)
[+] These authors contributed equally to this work.

[**] We are grateful to the following for support of this work: the European Research Council (ERC-2009-AdG 247143-QUANTIF) for funding to P.R.U., Marie Curie IEF (project 275450 "VISELCAT") under the EU's Seventh Framework Programme (FP7/2007-2013) for funding to S.C.S.L., and EPSRC for studentships to K.M. (MOAC/DTC) and A.N.P. (Analytical Fund EP/F064861/1e). We thank Dr. Alex Colburn for instrumentation designing and building and Petr Dudin for help with artwork preparation. Some equipment used in this research was obtained through Birmingham Science City with support from Advantage West Midlands and the European Regional Development Fund.

Supporting information for this article is available on the WWW under http://dx.doi.org/10.1002/anie.201200564.

forming a positionable and moveable nanoelectrochemical cell with the contacted area of the HOPG as the working electrode. The pipet itself never touches the sample. Because the pipet is tapered, high rates of (steady-state) diffusion can readily be achieved and, for charged species, mass transport can further be controlled through the bias between the two QRCEs.[12]

A potential bias (0.5 V) was applied between the two QRCEs and a small oscillation (20 nm peak amplitude, 233.6 Hz herein) was imposed on the *z*-position of the tip, giving rise to a conductance current across the meniscus with an alternating current (AC) component due to periodic changes in the meniscus height. Using the amplitude of the AC component as a set-point, the tip was scanned over the surface with a constant tip-to-substrate separation. By recording the currents between the QRCEs and at the substrate, and the positions of the piezoelectric positioners, simultaneous maps of local substrate electroactivity and topography are obtained. In this study, all SECCM maps cover 10×10 μm areas of HOPG (31 lines of 10 μm, scan rate 0.3 $\mu m\,s^{-1}$). A data point (an average of 512 measurements) was recorded every 30.1 ms, resulting in ca. 1100 points per line and over 30000 individual current measurements in an image. The contact diameter of the meniscus and the substrate was determined to be 220–320 nm (see Supporting Information, Section S2c), indicative of a SECCM spatial resolution an order of magnitude smaller than the typical μm-range step spacing on ZYA grade HOPG[10c] (used throughout this study, see Supporting Information). This allowed the basal plane to be probed in isolation, without influence of step edges.

SECCM maps obtained for the one-electron reduction of $[Ru(NH_3)_6]^{3+}$ (0.1 M KCl) on HOPG are shown in Figure 2. The topographical map of the surface obtained with SECCM (Figure 2a) clearly shows parallel steps (also evident from AFM, Figure 2e) across the surface, highlighting the outstanding ability of the technique to accurately track the surface and resolve nanoscale topographical features, despite a slight tilt (ca. 1.5°) on the sample. The steps are especially pronounced in Figure 2b, which shows the AC component of the conductance current (used as the feedback parameter). The sharp lines on this "error" map indicate a transient change in the feedback as the liquid meniscus comes into contact with a step, which we attribute to different wetting properties of the basal plane and the step edge.

A simultaneously recorded map of the surface redox activity at the reversible half-wave (formal) potential (−0.25 V vs. Ag/AgCl/0.1 M KCl), as determined by SECCM voltammetry (Figure S3a), shows the currents over the entire surface to be essentially constant at 30.9 ± 1.1 pA (1σ) (Figure 2c). The step sites show slightly higher currents (2–3%), but this is not necessarily an indicator of higher intrinsic activity, that is, current density. Most importantly, in the regions between the steps (where the electrolyte solution is only in contact with the basal surface), the current is at a constant (high) value.

Based on the observed current, an estimate of the standard ET rate constant can be made. The reversible voltammogram for $[Ru(NH_3)_6]^{3+}$ reduction shows a diffusion limited current of 16 pA (Figure S3a). By applying a potential bias of 0.5 V between the two QRCEs the limiting current increased by a factor of 4–5 due to migration (Section S2b). This corresponds to a high mass transport coefficient of ca. 0.5 $cm\,s^{-1}$, based on a 300 nm contact diameter. As the currents measured in the SECCM maps at the formal potential are ca. 50% of the transport-limited values, it is evident that the surface redox process measured during imaging is fast, and close to reversible, and we can put a conservative lower estimate on the standard ET rate constant of $> 0.5\ cm\,s^{-1}$ for $[Ru(NH_3)_6]^{3+}$ reduction on basal plane HOPG. That is to say, the process at HOPG would be entirely reversible to essentially all macroscopic electrochemical techniques, including past CV measurements, purely based on the activity of the basal surface, without needing to consider any activity of the step edges. This is in sharp contrast with the previously reported "negligible" activity of the basal surface.[1c,5]

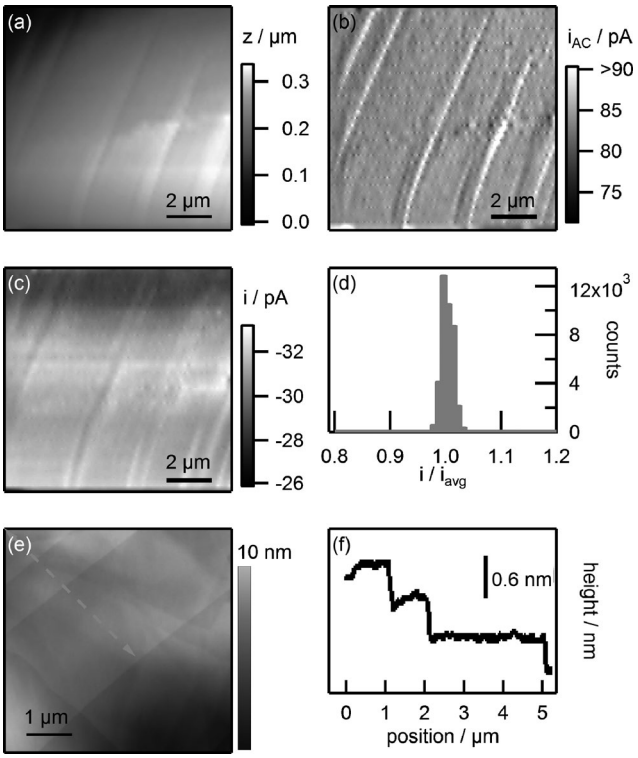

Figure 2. Reduction of 2 mM $[Ru(NH_3)_6]^{3+}$ at HOPG. SECCM maps of a) topography (*z*-piezo position), b) the AC component of the conductance current, and c) surface redox activity recorded at −0.25 V. d) Normalized activity histogram (see text). e) AFM image of the area of interest. f) Line scan along the arrow of the AFM image.

These findings are further validated by the other maps obtained simultaneously during imaging, most notably the consistency between all recorded trace and retrace images (Section S2b). The spread in redox activity over the image can be evaluated quantitatively (normalized for each line to minimize time effects), as shown by the histogram in Figure 2d. It can clearly be seen that the total spread in surface currents (ca. 30000 data points), is less than 5%, indicating a very homogeneously active surface. After performing SECCM measurements, the imaged area was characterized by AFM (Figure 2e) showing a step spacing ranging between

500 nm to 3 μm (Figure 2 f), with mainly monolayer steps present. As the lateral contact of SECCM is an order of magnitude smaller than the (average) step spacing, it is without doubt that during the electrochemical mapping the surface in contact with the electrolyte solution would mostly consist of only the HOPG basal plane. Thus, our data provide unambiguous evidence for the very high ET activity of the basal surface.

We also considered the electrochemical activity of $[Fe(CN)_6]^{4-/3-}$, a common benchmark redox system often used to study the electrochemical properties of HOPG,[1,3a,b,4,5,6a,7f] and related sp^2 carbon materials[1c,2h,3b] and originally employed to draw conclusions regarding the relative electroactivity of the basal plane and step sites. SECCM results for the oxidation of 2 mM $[Fe(CN)_6]^{4-}$ (0.1 M KCl) on HOPG at 0.25 V (vs. Ag/AgCl/0.1 M KCl) are shown in Figure 3. The potential was chosen based on voltammograms recorded on freshly cleaved HOPG and on HOPG after exposure to air for 1 h, being the timescale of a SECCM measurement (Figure S3). The limiting current in the absence of migration was 15 pA and 4–5 times larger with the applied potential between the QRCEs. The resulting electroactivity map (Figure 3 a) shows a clear side-on "V-shaped" feature consistent with the step sites on the HOPG surfaces (see AFM data, Figure 3 e and f). Interestingly, in contrast to the reduction of $[Ru(NH_3)_6]^{3+}$, these steps display lower currents than the basal plane. Furthermore, a clear deactivation of the overall surface is seen during the timescale of the image (from bottom to top). This decrease is especially clear from the average current of each line (Figure 3 b), which dropped by 35% over the course of the image from 69 pA (where the reaction is rapid and close to reversible) to 45 pA. It should again be emphasized that the other simultaneously obtained maps (Section S2b) indicate a stable meniscus contact, and that the meniscus is moved during the scan to areas which have not been exposed to the electrolyte solution. This deterioration has been observed in extensive related experiments in our lab and is due to a combination of issues which we expand on briefly below. For this study, to probe the relative reactivity of basal and step sites in isolation of time effects, a current distribution was obtained by normalizing each line with the average current of that line (Figure 3 c and d). Most of the sites display similar activity (within 10%), although a slight tailing towards lower activity can be seen. Looking at the normalized current SECCM map, the regions of below average current are assigned to the step sites. Furthermore, the difference between the step site and basal plane reactivity appears to increase with time, giving rise to the broad distribution of activity in Figure 3 d between 0.7 and 1. This increasing difference could be indicative of a preferential deactivation of step sites over basal plane sites with time, similar to metal electrodes.[13] Based on these data, we can only conclude that the HOPG basal plane is highly active for the $[Fe(CN)_6]^{4-/3-}$ benchmark system, being close to reversible initially, albeit with some complications. This contrasts markedly with previous reports, and it should be noted that previously reported ET standard rate constants (10^{-5}–10^{-9} cm s^{-1}, averaged for the surface[3a,6b,c] or 10^{-9} cm s^{-1}, extrapolated for the basal surface[1c,3c]) would have yielded negligible (close to zero) currents at the potential of our high mass transport rate studies. Furthermore, it should be noted that the ET rate constants reported here are consistent with predictions from Marcus theory (> 1 cm s^{-1}).[1b]

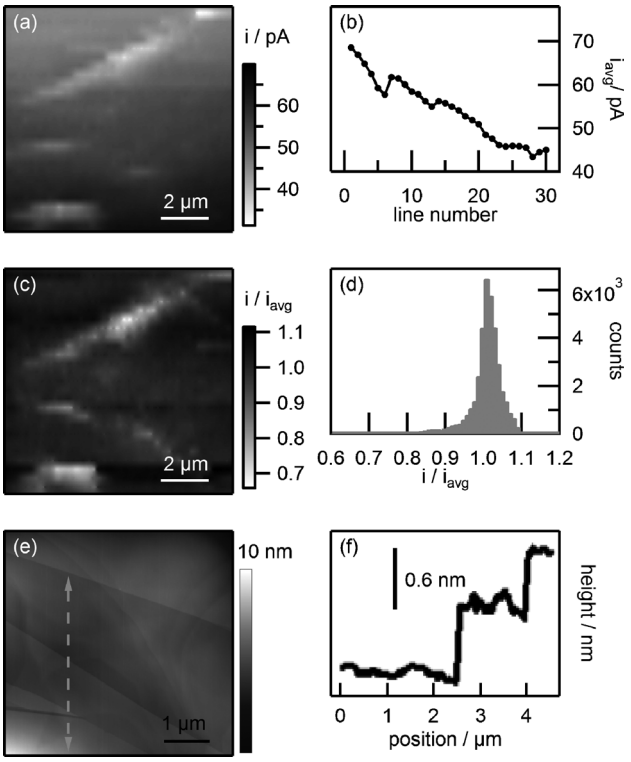

Figure 3. Oxidation of 2 mM $[Fe(CN)_6]^{4-}$ at HOPG. a) SECCM surface redox activity map recorded at 0.25 V. b) Average current of each line scan. c) Normalized SECCM surface redox activity map (see text). d) Normalized activity histogram (see text). e) AFM image of the area of interest. f) Line scan along the arrow of the AFM image.

Although SECCM clearly illustrates the HOPG basal plane to be highly active, the different currents obtained when imaging directly over step sites is interesting and merits some discussion. We believe this effect is due to the heterogeneous properties of the basal surface versus step edges, resulting in different (nanoscale) wetting and adsorption processes: the excess negative charge on the HOPG step edges[14] could draw in the positively charged $[Ru(NH_3)_6]^{3+}$ through electrostatic interaction, causing a slight spreading of the meniscus, thereby increasing the contact area. This finding is supported by an increase in conductance current (Figure S2.1), which is a good indicator for variances in meniscus size, and the transient surges in the AC (Figure 2 b). Due to the increased contact area, the surface current increases, even if the intrinsic activity remains unchanged going over a step edge. In contrast, for the negatively charged $[Fe(CN)_6]^{4-}$ species, we see the conductance current decrease, suggesting that the meniscus slightly contracts when going over a step site (Figure S2.2). These data highlight the high information content of SECCM for structure–function imaging of surfaces and interfaces.

Finally, the question remains why our main finding, namely that the (freshly exposed) basal plane of HOPG

displays considerable electroactivity, differs from previous studies which have come to the opposite conclusion.[1,2g,3] In this respect, it should be noted that fast ET for $[Fe(CN)_6]^{4-/3-}$ and $[Ru(NH_3)_6]^{3+/2+}$ on freshly cleaved HOPG has been reported by others from CV measurements,[7g,15] but often discarded as "very defective" based on the current models, without any further surface characterization. Furthermore, the surface of HOPG is known to be very sensitive to adsorption: for example, exposure of HOPG to organic solvents, can lead to significant alteration of its surface properties.[15] In addition, as shown here, exposure to air for less than an hour after cleaving leads to a decrease in ET rates at the basal surface. Finally, voltammetric studies of $[Fe(CN)_6]^{4-/3-}$ on other electrodes have identified adsorption and surface blocking effects.[16] All of these factor need to be taken into account in the design of experiments to probe HOPG electrode surface kinetics. The results presented herein clearly represent the intrinsic electrochemical properties of (pristine) HOPG. Separately, we are carrying out an in-depth study to understand and explain time-dependent surface effects on HOPG electrodes and will report on this shortly.

In summary, SECCM has allowed us to study ET at basal plane HOPG under conditions of very high mass transport and high spatial resolution, and where the liquid probe makes a series of fresh measurements across the surface. We have been able to isolate the response of the pristine basal plane (directly after cleaving, thus reflecting the intrinsic material properties), and show unambiguously that ET is fast (close to reversible) for the two most studied redox couples. This new view—which overturns more than two decades of past research[1,3–8]—not only impacts our understanding of the electroactivity of HOPG, but potentially the properties of related sp^2 materials, such as carbon nanotubes and graphene, illustrating the importance of our findings. Our studies also demonstrate the significant potential of SECCM as a new nanoscale probe of electrochemical and interfacial processes.

Received: January 20, 2012
Revised: February 27, 2012
Published online: April 5, 2012

Keywords: electrochemistry · graphite · scanning electrochemical cell microscopy · scanning probe microscopy · surface analysis

[1] a) I. Dumitrescu, P. R. Unwin, J. V. Macpherson, *Chem. Commun.* **2009**, 6886–6901; b) R. L. McCreery, *Chem. Rev.* **2008**, *108*, 2646–2687; c) C. E. Banks, T. J. Davies, G. G. Wildgoose, R. G. Compton, *Chem. Commun.* **2005**, 829–841; d) M. Pumera, *Chem. Soc. Rev.* **2010**, *39*, 4146–4157.

[2] a) M. Zhou, Y. M. Zhai, S. J. Dong, *Anal. Chem.* **2009**, *81*, 5603–5613; b) Y. Wang, Z. Q. Shi, Y. Huang, Y. F. Ma, C. Y. Wang, M. M. Chen, Y. S. Chen, *J. Phys. Chem. C* **2009**, *113*, 13103–13107; c) L. H. Tang, Y. Wang, Y. M. Li, H. B. Feng, J. Lu, J. H. Li, *Adv. Funct. Mater.* **2009**, *19*, 2782–2789; d) C. S. Shan, H. F. Yang, J. F. Song, D. X. Han, A. Ivaska, L. Niu, *Anal. Chem.* **2009**, *81*, 2378–2382; e) F. Chen, Q. Qing, J. L. Xia, J. H. Li, N. J. Tao, *J. Am. Chem. Soc.* **2009**, *131*, 9908–9909; f) S. Alwarappan, A. Erdem, C. Liu, C. Z. Li, *J. Phys. Chem. C* **2009**, *113*, 8853–8857; g) W. Li, C. Tan, M. A. Lowe, H. D. Abruna, D. C. Ralph, *ACS Nano* **2011**, *5*, 2264–2270; h) A. T. Valota, I. A. Kinloch, K. S. Novoselov, C. Casiraghi, A. Eckmann, E. W. Hill, R. A. W. Dryfe, *ACS Nano* **2011**, *5*, 8809–8815.

[3] a) R. J. Bowling, R. T. Packard, R. L. McCreery, *J. Am. Chem. Soc.* **1989**, *111*, 1217–1223; b) X. B. Ji, C. E. Banks, A. Crossley, R. G. Compton, *ChemPhysChem* **2006**, *7*, 1337–1344; c) T. J. Davies, R. R. Moore, C. E. Banks, R. G. Compton, *J. Electroanal. Chem.* **2004**, *574*, 123–152; d) C. Y. Lee, A. M. Bond, *Anal. Chem.* **2009**, *81*, 584–594.

[4] K. R. Kneten, R. L. McCreery, *Anal. Chem.* **1992**, *64*, 2518–2524.

[5] a) C. E. Banks, R. R. Moore, T. J. Davies, R. G. Compton, *Chem. Commun.* **2004**, 1804–1805; b) T. J. Davies, M. E. Hyde, R. G. Compton, *Angew. Chem.* **2005**, *117*, 5251–5256; *Angew. Chem. Int. Ed.* **2005**, *44*, 5121–5126.

[6] a) K. K. Cline, M. T. McDermott, R. L. McCreery, *J. Phys. Chem.* **1994**, *98*, 5314–5319; b) R. J. Rice, R. L. McCreery, *Anal. Chem.* **1989**, *61*, 1637–1641; c) M. T. McDermott, K. Kneten, R. L. McCreery, *J. Phys. Chem.* **1992**, *96*, 3124–3130.

[7] a) R. J. Bowling, R. L. McCreery, C. M. Pharr, R. C. Engstrom, *Anal. Chem.* **1989**, *61*, 2763–2766; b) P. H. Chen, M. A. Fryling, R. L. McCreery, *Anal. Chem.* **1995**, *67*, 3115–3122; c) M. T. McDermott, R. L. McCreery, *Langmuir* **1994**, *10*, 4307–4314; d) R. S. Robinson, K. Sternitzke, M. T. McDermott, R. L. McCreery, *J. Electrochem. Soc.* **1991**, *138*, 2412–2418; e) R. R. Moore, C. E. Banks, R. G. Compton, *Anal. Chem.* **2004**, *76*, 2677–2682; f) C.-Y. Lee, S.-X. Guo, A. M. Bond, K. B. Oldham, *J. Electroanal. Chem.* **2008**, *615*, 1–11; g) J. K. Kariuki, M. T. McDermott, *Langmuir* **1999**, *15*, 6534–6540.

[8] a) K. Ray, R. L. McCreery, *Anal. Chem.* **1997**, *69*, 4680–4687; b) H. Chang, A. J. Bard, *Langmuir* **1991**, *7*, 1143–1153.

[9] a) S. C. S. Lai, P. V. Dudin, J. V. Macpherson, P. R. Unwin, *J. Am. Chem. Soc.* **2011**, *133*, 10744–10747; b) N. Ebejer, M. Schnippering, A. W. Colburn, M. A. Edwards, P. R. Unwin, *Anal. Chem.* **2010**, *82*, 9141–9145.

[10] a) T. Suter, H. Böhni, *Electrochim. Acta* **1997**, *42*, 3275; b) A. Hassel, M. Lohrengel, *Electrochim. Acta* **1997**, *42*, 3327; c) C. G. Williams, M. A. Edwards, A. L. Colley, J. V. Macpherson, P. R. Unwin, *Anal. Chem.* **2009**, *81*, 2486–2495.

[11] a) C. G. Zoski, *Handbook of Electrochemistry*, Elsevier, **2006**; b) R. G. Compton, C. E. Banks, *Understanding Voltammetry*, Imperial College Press, **2011**.

[12] M. E. Snowden, A. G. Güell, S. C. S. Lai, K. McKelvey, N. Ebejer, M. A. O'Connell, A. W. Colburn, P. R. Unwin, *Anal. Chem.* **2012**, *84*, 2483–2491.

[13] a) P. J. Feibelman, S. Esch, T. Michely, *Phys. Rev. Lett.* **1996**, *77*, 2257–2260; b) T. Zambelli, J. Wintterlin, J. Trost, G. Ertl, *Science* **1996**, *273*, 1688–1690.

[14] R. Koestner, Y. Roiter, I. Kozhinova, S. Minko, *J. Phys. Chem. C* **2011**, *115*, 16019–16026.

[15] Y. Liu, M. S. Freund, *Langmuir* **2000**, *16*, 283–286.

[16] C. M. Pharr, P. R. Griffiths, *Anal. Chem.* **1997**, *69*, 4673–4679.

